

# Interwoven Metal-Organic Framework on a Periodic Minimal Surface with Extra-Large Pores

Banglin Chen,<sup>1</sup> M. Eddaoudi,<sup>1</sup> S. T. Hyde,<sup>2</sup> M. O'Keeffe,<sup>3</sup>  
O. M. Yaghi<sup>1\*</sup>

Interpenetration (catenation) has long been considered a major impediment in the achievement of stable and porous crystalline structures. A strategy for the design of highly porous and structurally stable networks makes use of metal-organic building blocks that can be assembled on a triply periodic *P*-minimal geometric surface to produce structures that are interpenetrating—more accurately considered as interwoven. We used 4,4',4''-benzene-1,3,5-triyl-tribenzoic acid ( $H_3\text{BTB}$ ), copper(II) nitrate, and *N,N'*-dimethylformamide (DMF) to prepare  $\text{Cu}_3(\text{BTB})_2(\text{H}_2\text{O})_3\cdot(\text{DMF})_9(\text{H}_2\text{O})_2$  (MOF-14), whose structure reveals a pair of interwoven metal-organic frameworks that are mutually reinforced. The structure contains remarkably large pores, 16.4 angstroms in diameter, in which voluminous amounts of gases and organic solvents can be reversibly sorbed.

Interlocking, or catenation, on the molecular level has captured the imagination of scientists because of its potential for constructing complex biological and synthetic assemblies. Many organic (*1*, *2*) and DNA (*3*, *4*) catenanes with linked macrocyclic molecules have now been described. The first example of linked protein rings was recently reported in the capsid of bacteriophage HK97; in this material, 72 rings are interlocked to form a closed surface in a manner likened to “chain mail” (*5*). Periodic structures with interpenetrating nets (*1*, *6*) are also catenated in the sense that the links of one net pass through the rings of the other, and vice versa. This structural feature is widely believed to have a negative impact on the size and accessibility of pores in microporous materials (*7*). Here, we identify a type of net in which the vertices fall on a periodic minimal surface, and for which interpenetration is more appropriately considered interweaving, so that the structure forms an infinite periodic chain mail. As an exemplar of this design principle, we describe the synthesis, structure, and sorption properties of a porous metal-organic framework (MOF) that has the largest pores of any stable occurrence of such a compound reported to date.

Our design strategy is to link symmetrical secondary building units (SBUs) and thus produce structures based on the simplest

(most regular) nets (*8*). In the case of 3- and 4-connected nets, these are the cubic structures named for  $\text{SrSi}_2$  and diamond, respectively (*8*, *9*). In structures produced by interpenetration of pairs of these nets, the vertices of each net are maximally displaced from the periodic minimal surface (*G* and *D*, respectively), dividing the two nets (*10*) such that the vertices of one net fill the voids of the other structure (*11*). In contrast, the simplest and most symmetrical (3,4)-connected net with square coordination is that named for  $\text{Pt}_3\text{O}_4$  (*8*, *9*); in this net, the vertices fall on the *P*-minimal surface described below. If a second such net is displaced by  $\frac{1}{2}, \frac{1}{2}, \frac{1}{2}$  lattice units from the first, the 4-connected (*Pt*) vertices avoid each other with both sets on the surface, whereas the 3-connected vertices (*O*) coincide. To make such an interpenetrating but nonintersecting structure, it is necessary to displace the 3-connected vertices from their positions; if this is done, an interwoven structure will be obtained with a labyrinth of interconnected pores.

To implement this design, we use the binuclear copper carboxylate “paddle wheel” (*12*) as a square SBU, and the 1, 3, and 5 positions of a benzene ring as a triangular SBU. These units must be joined by long linkers, in our case phenyl groups, to achieve a large open structure; thus, the carboxylic acid is 4,4',4''-benzene-1,3,5-triyl-tribenzoic acid ( $H_3\text{BTB}$ ) and the framework has composition  $\text{Cu}_3(\text{BTB})_2$ . The linker was subjected to reactions that give the paddle-wheel metal carboxylate unit: Reaction of  $H_3\text{BTB}$  (0.23 g, 0.052 mmol) with  $\text{Cu}(\text{NO}_3)_2 \cdot 2.5\text{H}_2\text{O}$  (0.065 g, 0.28 mmol) in a solvent mixture of ethanol (3 ml), *N,N'*-dimethylformamide

(DMF) (3 ml), and water (2 ml) in the presence of excess pyridine (0.62 mmol) at 65°C for 1 day produced large green cubic crystals in high yield. This product is stable in air and insoluble in water and common organic solvents; it was formulated as  $\text{Cu}_3(\text{BTB})_2(\text{H}_2\text{O})_3\cdot(\text{DMF})_9(\text{H}_2\text{O})_2$  (hereafter MOF-14) on the basis of elemental microanalysis (*13*).

Single crystals isolated from the reaction product were examined by x-ray diffraction (XRD) (*13*). The structure was found to be constructed of an identical pair of frameworks, each having BTB units linking Cu(II) ions into the expected paddle-wheel cluster motif. Each BTB is linked to three such clusters and each cluster to four BTB units, resulting in an augmented (3,4)-connected net with the  $\text{Pt}_3\text{O}_4$  topology, in which squares replace the 4-connected vertices and triangles replace the 3-connected vertices (Fig. 1, A to C). The triangular units (representing the central benzene ring of the acid) are displaced from each other by 3.68 Å (a distance consonant with strong  $\pi$ - $\pi$  interactions) and bowed by 0.86 Å to admit the interweaving of the two subunits (Fig. 1D), where additional six C-H $\cdots$  $\pi$  interactions (3.69 Å) between all 2-connected benzene rings mutually hold the BTB units close together (*14*). The two discrete nets in the MOF-14 structure are displaced from one another by  $\frac{1}{2}, \frac{1}{2}, \frac{1}{2}$  and separated by a continuous hyperbolic surface. Although the two nets are separated by a continuous surface, the rings of one net are penetrated by links of the other so that they are truly catenated (Fig. 1E). The interweaving allows mutual reinforcement of the exceptionally large BTB moieties, which alone would be expected to be insufficiently rigid to sustain an open framework.

The separating surface is the *P*-minimal surface, one of the simplest triply periodic minimal surfaces in Euclidean space; it partitions space into two interpenetrating labyrinths, each consisting of six orthogonal channels meeting at sites of a primitive cubic lattice (Fig. 2). The *P*-surface is relevant to many inorganic crystal structures, as well as liquid crystalline mesophases of amphiphiles in water, lipids *in vivo*, and copolymers (*10*). In the MOF-14 structure, one net is displaced to one side of the *P*-surface and the other to the other side by the same amount.

Despite interpenetration, the interwoven pair of frameworks in MOF-14 occupy only a small fraction of the available space in the crystal, which contains large cavities. The nearest neighbors of the center of each internal cavity are 216 C atoms at a distance of 9.88 to 11.85 Å, so that after allowing 1.7 Å for the van der Waals radius of carbon, a sphere 16.4 Å in diameter can fit inside each cavity. This cavity size is substantially larger than that of the noninterpenetrated MOF-5 (*15*). In the as-prepared material, the cavity is

<sup>1</sup>Department of Chemistry, University of Michigan, Ann Arbor, MI 48109, USA. <sup>2</sup>Department of Applied Mathematics, Australian National University, Canberra, Australia. <sup>3</sup>Department of Chemistry, Arizona State University, Tempe, AZ 85287, USA.

\*To whom correspondence should be addressed. E-mail: oyaghi@umich.edu

## REPORTS

occupied by at least 36 DMF and eight water guests (a total of 152 non-hydrogen atoms), in addition to 12 water ligands that are axially bound to copper. The space occupied by guests alone represents 67% of the cell volume or  $13,166 \text{ \AA}^3$  per unit cell. The aperture

joining two cavities has a dimension of  $7.66 \text{ \AA}$  by  $14.00 \text{ \AA}$ . Indeed, organic vapor and gas sorption studies indicate that this space is accessible to incoming guest species.

Evidence of high guest mobility and structural stability was obtained by placing a sam-

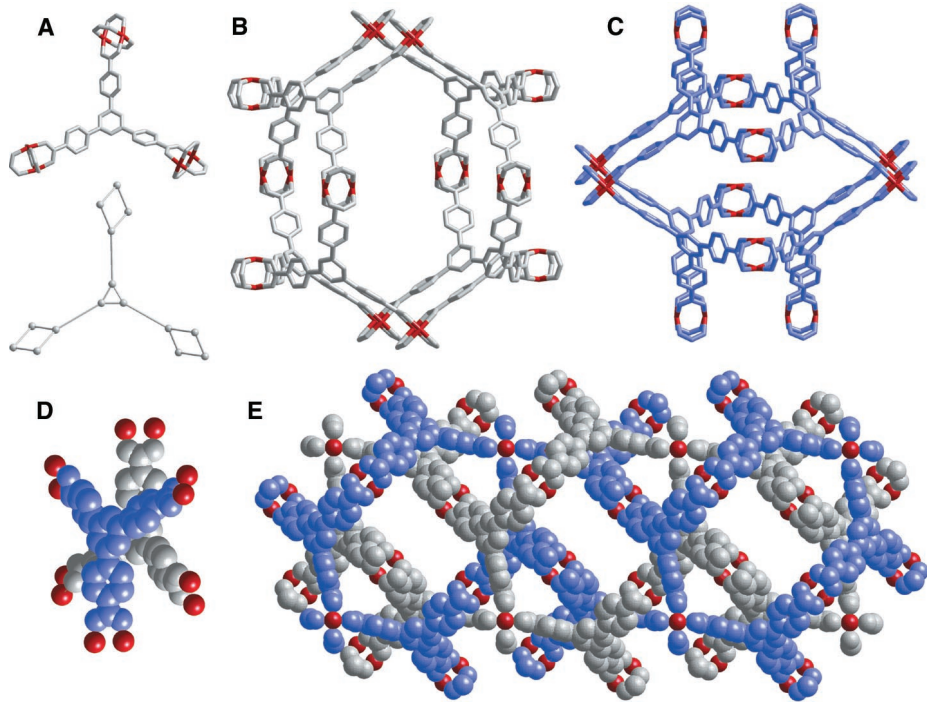
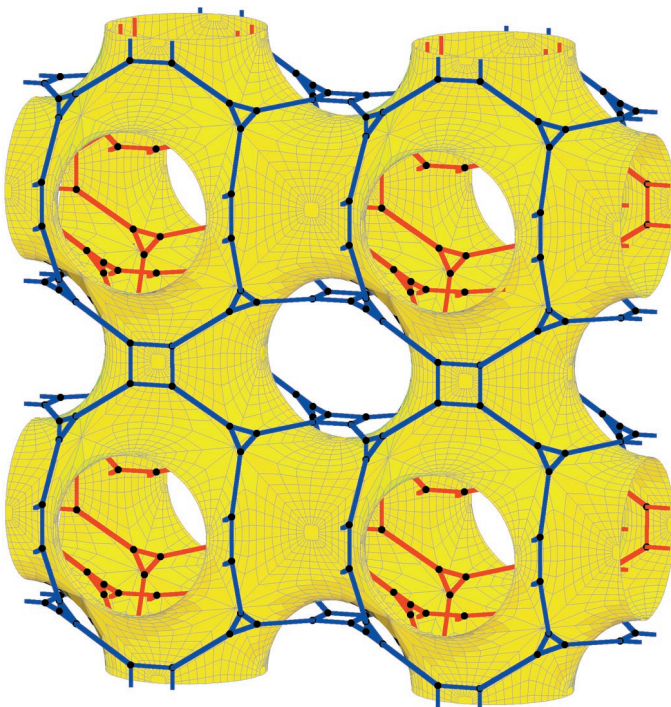


**Fig. 1.** Single-crystal structure of  $\text{Cu}_3(\text{BTB})_2(\text{H}_2\text{O})_3 \cdot (\text{DMF})_3(\text{H}_2\text{O})_2$  (MOF-14) composed of (A) square paddle-wheel and triangular BTB SBUs, which assemble into (B and C) a pair of augmented  $\text{Pt}_3\text{O}_4$  nets that are held together by (D) numerous  $\pi$ - $\pi$  and C-H... $\pi$  interactions to yield (E) a pair of interwoven three-dimensional porous frameworks. Cu, red; C, gray or blue atoms not linked directly to Cu; O, gray atoms linked directly to Cu. Guests, water ligands, and hydrogen atoms are omitted for clarity.

**Fig. 2.** Two MOF-14 frameworks (blue and red) interwoven about a  $P$ -minimal surface without intersecting the surface.



ple (50.4 mg) of MOF-14 in an electrogravimetric balance under  $10^{-5}$  torr at room temperature. After 40 hours, a weight loss of 38.5% was observed, which is equivalent to the loss of virtually all guests (calculated 38.5%) to produce  $\text{Cu}_3(\text{BTB})_2(\text{H}_2\text{O})_3$  (evacuated MOF-14), as confirmed by elemental analysis. Thermogravimetric analysis performed in inert atmosphere showed that evacuated MOF-14 is stable up to  $250^\circ\text{C}$ . The rigidity and permanent porosity of the evacuated framework was confirmed by gas sorption isotherm experiments (16). The  $\text{N}_2$  sorption revealed a reversible type I isotherm (Fig. 3). The same sorption behavior was observed for Ar, CO,  $\text{CH}_4$ , and organic vapors such as  $\text{CH}_2\text{Cl}_2$ ,  $\text{CCl}_4$ ,  $\text{C}_6\text{H}_6$ ,  $\text{C}_6\text{H}_{12}$ , and *m*-xylene. Similar to those of most zeolites, the isotherms are reversible and show no hysteresis upon desorption of gases from the pores. Using the Dubinin-Radushkovich equation, pore volumes near  $0.53 \text{ cm}^3/\text{g}$  were found for all adsorbates, which indicates that the pores are uniform. For a monolayer coverage of  $\text{N}_2$  (which may not be strictly correct with such large cavities), we estimate the apparent Langmuir surface area to be  $1502 \text{ m}^2/\text{g}$ . The pore volume and surface area determined for MOF-14 are well beyond those observed for the most porous crystalline zeolites and related molecular sieves (17).

Guest exchange studies indicate that MOF-14 also maintains its structural integrity in solution. In a typical experiment, an as-synthesized solid sample of MOF-14 was immersed in an organic solvent and allowed to stand for a short period of time (5 to 60 min) at room temperature, and the solid was then separated and analyzed for the inclusion of the new solvent guest (13). The powder XRD patterns of all inclusion complexes of MOF-14 indicate highly crystalline products with patterns essentially identical to that of the as-synthesized material. An XRD study performed on crystals that lost 72% of the guest content shows no change in cell parameters, with the overall structure of MOF-14 fully retained (13). These data and the gas sorption isotherms demonstrate that, unlike

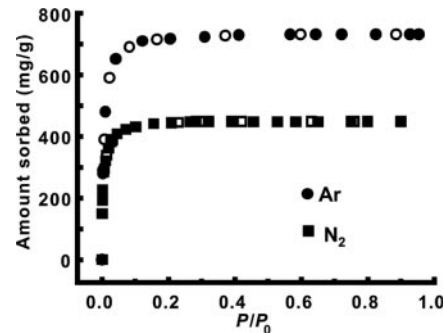


**Fig. 3.** Gas sorption isotherms for  $\text{N}_2$  and Ar, measured at  $78 \text{ K}$ . Filled symbols, sorption; open symbols, desorption;  $P_0 = 1 \text{ atm}$ .

## REPORTS

other interpenetrating structures, interweaving in MOFs with a framework conforming closely to a periodic minimal surface can produce materials with large cavities, exceptionally high pore volume, and permanent porosity, as exemplified by MOF-14.

### References and Notes

1. J. P. Sauvage, C. Dietrich-Buchecker, Eds., *Molecular Catanes, Rotaxanes and Knots* (Wiley-VCH, New York, 1999).
2. F. M. Raymo, J. F. Stoddart, *Chem. Rev.* **99**, 1643 (1999).
3. N. C. Seeman, *Annu. Rev. Biophys. Biomol. Struct.* **27**, 225 (1998).
4. J. J. Storhoff, C. A. Mirkin, *Chem. Rev.* **99**, 1849 (1999).
5. W. R. Wikoff *et al.*, *Science* **289**, 2129 (2000).
6. S. R. Batten, R. Robson, *Angew. Chem. Int. Ed.* **37**, 1460 (1998).
7. For the design of intergrown nets with optimal porosity, see T. M. Reineke, M. Eddaoudi, D. Moler, M. O'Keeffe, O. M. Yaghi, *J. Am. Chem. Soc.* **122**, 4843 (2000).
8. M. O'Keeffe, M. Eddaoudi, H. Li, T. Reineke, O. M. Yaghi, *J. Solid State Chem.* **152**, 3 (2000).
9. M. O'Keeffe, B. G. Hyde, *Crystal Structures I: Patterns and Symmetry* (Mineralogical Society of America, Washington, DC, 1996).
10. S. T. Hyde *et al.*, *The Language of Shape* (Elsevier, Amsterdam, 1997).
11. The vertices of two interpenetrating diamond nets form the dense body-centered cubic array as in the structures of NaTl compounds [see, e.g., (8)].
12. For a recent example and references, see B. Chen *et al.*, *J. Am. Chem. Soc.* **122**, 11559 (2000).
13. Details of the elemental analysis and crystal structures for as-synthesized and evacuated MOF-14 [ $\text{Im} \overline{\text{3}}$ ,  $a = 26.946(2)$  and  $26.919(1) \text{ \AA}$ , respectively] and the elemental analysis of solvent-exchanged MOF-14 are available at *Science Online* ([www.sciencemag.org/cgi/content/full/291/5506/1021/DC1](http://www.sciencemag.org/cgi/content/full/291/5506/1021/DC1)). X-ray coordinates have been deposited with the Cambridge Data Bank.
14. E. Weber *et al.*, *J. Chem. Soc. Perkin Trans. II* **1988**, 1251 (1988).
15. H. Li, M. Eddaoudi, M. O'Keeffe, O. M. Yaghi, *Nature* **402**, 276 (1999).
16. M. Eddaoudi, H. Li, O. M. Yaghi, *J. Am. Chem. Soc.* **122**, 1391 (2000).
17. D. W. Breck, *Zeolite Molecular Sieves* (Wiley, New York, 1974).
18. Supported by NSF grants DMR-9804817 (M.O.K.) and CHE-9980469 (O.M.Y.) and by the U.S. Department of Energy (O.M.Y.). We thank S. Ramsden for production of Fig. 2.

16 October 2000; accepted 21 December 2000

## Surface-Directed Liquid Flow Inside Microchannels

Bin Zhao,<sup>1</sup> Jeffrey S. Moore,<sup>1\*</sup> David J. Beebe<sup>2</sup>

**Self-assembled monolayer chemistry was used in combination with either multistream laminar flow or photolithography to pattern surface free energies inside microchannel networks. Aqueous liquids introduced into these patterned channels are confined to the hydrophilic pathways, provided the pressure is maintained below a critical value. The maximum pressure is determined by the surface free energy of the liquid, the advancing contact angle of the liquid on the hydrophobic regions, and the channel depth. Surface-directed liquid flow was used to create pressure-sensitive switches inside channel networks. The ability to confine liquid flow inside microchannels with only two physical walls is expected to be useful in applications where a large gas-liquid interface is critical, as demonstrated here by a gas-liquid reaction.**

Manipulating gas and liquid fluids within networks of microchannels is crucial in the design and fabrication of microfluidic devices for applications in bioassays, microreactors, and chemical and biological sensing (1). Many techniques including mechanical pumping (2), electro-osmotic flow (3, 4), electrowetting (5), electrochemistry (6), and thermocapillary pumping (7, 8) have been used to pump, transport, position, and mix liquid samples. Surface properties, especially wetting, have significant effects on liquid behavior (9–11) when the system is reduced to a submillimeter scale. For example, surface effects are the basis of capillary pumping (12) and light-driven motion of liquids on a photoresponsive surface (13). Recent studies on patterned surfaces (14–16) revealed interesting phenomena that can be exploited to control liquid motions in microfluidic devices. Here, we report a simple method, based on patterning surface free energies, to manipu-

late liquid flow within channel networks. Aqueous solutions are confined to hydrophilic pathways, creating a large gas-liquid interface that makes gas-liquid reactions practical in microfluidic systems.

Patterning hydrophobic and hydrophilic regions inside microchannels typically requires modifying the surface in selected areas first, and then aligning and bonding substrates to form microchannel networks (11). This process consists of a series of complicated and time-consuming steps. We have patterned surface free energies inside channel networks by combining multistream liquid laminar flow and self-assembled monolayer (SAM) chemistry. The entire process is completed quickly (within several minutes) and in situ. Liquid flow inside microchannels is laminar, meaning that multiple liquid streams can flow side-by-side without turbulent mixing, allowing good spatial control (17). Multistream liquid laminar flow has been used to fabricate diffusion-based extractors, various microstructures, and cell patterns inside pre-formed capillaries (17–20). Deposition of SAMs is a simple method to modify surface wetting properties of a variety of materials (21–23). By controlling the water content in the solvent, SAMs of trichlorosilanes can be

formed on silica substrates in a short period of time (i.e., several minutes or even less) (22, 24).

The channels used here were made from glass substrates and glass cover slips (25). A stream of pure hexadecane and a stream of octadecyltrichlorosilane (OTS) solution in hexadecane were brought together in channels by syringe pumps, and the laminar flow was maintained for 2 to 3 min (26). SAMs formed on both the top and bottom of the channels in the area containing the trichlorosilane solution. The other surfaces remained hydrophilic ( $\theta_p \sim 0^\circ$ ;  $\theta_p$  is the water advancing contact angle on a polar surface). A series of patterned surfaces were fabricated as shown in Fig. 1, A to D. Once patterned, aqueous solutions flowed only on hydrophilic pathways (Fig. 1, E to H, corresponding to Fig. 1, A to D, respectively) when the pressure was maintained below a critical value. If minor disturbances caused the liquid to flow into the hydrophobic region, the liquid gradually retreated to the hydrophilic pathway. When the pressure exceeded a critical value, the solution crossed the boundary between hydrophilic and hydrophobic regions. Using these patterned surfaces, we could transport liquids from one reservoir to another along the specified pathway (Fig. 1F), and could flow two streams side-by-side separated by a gas membrane, allowing volatile compounds to be transported from one stream to the other (Fig. 1, E, G, and H). Because there are no physical walls on the sides of the liquid stream, we refer to the stream as being confined by “virtual” walls.

A liquid stream will rupture the virtual wall when the angle of curvature of the liquid at the hydrophilic-hydrophobic boundary ( $\theta_b$ ) equals the advancing contact angle of the liquid on the nonpolar surface ( $\theta_n$ ) (Fig. 2A). When the water surface is curved, there is a pressure drop across the liquid-gas interface due to surface free energy. The pressure on the concave side is always greater than the pressure on the convex side, as described by the Young-Laplace equation  $\Delta P = \gamma(1/R_1 +$

<sup>1</sup>The Beckman Institute for Advanced Science and Technology, University of Illinois at Urbana-Champaign, Urbana, IL 61801, USA. <sup>2</sup>Department of Bio-medical Engineering, University of Wisconsin-Madison, Madison, WI 53706, USA.

\*To whom correspondence should be addressed. E-mail: moore@scs.uiuc.edu